Proceedings of the ASME 2010 3rd Joint US-European Fluids Engineering Summer Meeting and 8th International Conference on Nanochannels, Microchannels, and Minichannels
FEDSM-ICNMM2010
August 1-5, 2010, Montreal, Canada

FEDSM-ICNMM2010-31070

ENTROPY GENERATION IN THERMALLY DEVELOPING LAMINAR FORCED CONVECTION THROUGH A SLIT MICROCHANNEL

Arman Sadeghi
Ph.D. Student of Mechanical Engineering
Sharif University of Technology, Tehran, Iran

Mostafa Baghani
Ph.D. Candidate of Mechanical Engineering
Sharif University of Technology, Tehran, Iran

Mohammad Hassan Saidi*
Professor of Mechanical Engineering
Sharif University of Technology, Tehran, Iran, P.O. Box: 11155-9567

ABSTRACT

The issue of entropy generation in laminar forced convection of a Newtonian fluid through a slit microchannel is analytically investigated by taking the viscous dissipation effect, the slip velocity and the temperature jump at the wall into account. Flow is considered to be hydrodynamically fully developed but thermally developing. The energy equation is solved by means of integral transform. The results demonstrate that to increase Knudsen number is to decrease entropy generation, while the effect of increasing values of Brinkman number and the group parameter is to increase entropy generation. Also it is disclosed that in the thermal entrance region the average entropy generation number over the cross section of channel is an increasing function of axial coordinate.

Keywords: Microchannel; Slip flow; Viscous dissipation; Knudsen number; Entropy generation; Bejan number

1 INTRODUCTION

Microchannels with dimensions ranging from 100 μm to fractions of 1 μm have found applications for use in the cooling of integrated circuits (ICs), biochemical applications, microelectromechanical systems (MEMS) and cryogenics. This characteristic geometric scale is comparable with the gas mean free path, which at standard atmospheric condition is about 100 *nm*. In this case, the gas flow cannot be modeled based on the continuum hypothesis, since the rarefaction effects are important. The deviation of the state of the gas from continuum behavior is measured by the Knudsen Number (Kn), which is defined as $Kn = \lambda/D_h$, where λ is the mean free path of gas molecules and D_h is the channel hydraulic diameter. Based on a definition given by Beskok and Karniadakis [1], gas flow can be classified as one of four regimes according to its Knudsen number. In the slip flow regime which corresponds to $10^{-3} \leq Kn \leq 0.1$, deviations from the state of continuum are relatively small and the Navier-Stokes equations are still valid. The rarefaction effect can be modeled through the partial slip at the wall using slip boundary conditions which can be determined using kinetic theory of gases. The experiments conducted by Liu et al. [2] and Hsieh et al. [3] on the transport of gases through microchannels confirm that Navier-Stokes equations subject to first order slip boundary conditions can be used to obtain flow characteristics in micronsize devices.

Several research efforts have presented the analytical solutions for laminar slip flow forced convection through simple microgeometries. Aydin and Avci [4,5] theoretically investigated the steady, laminar, fully developed forced convection in a microtube and microduct between two parallel plates for both boundary conditions of constant wall temperature and constant wall heat flux. Heat transfer characteristics of hydrodynamically and thermally fully developed laminar rarefied gas flow in annular microducts with constant wall heat fluxes have been studied by Duan and Muzychka [6]. They have performed the analysis by combining the solutions of two sub problems consisting of a microchannel with one wall being adiabatic and the other having constant heat flux. Tunc and Bayazitoglu [7] studied both hydrodynamically and thermally fully developed slip flow in rectangular microducts. The H2 type boundary condition, constant axial and peripheral heat flux, was applied at the channel walls.

The problem of hydrodynamically fully developed and thermally developing flow in a channel, with the assumptions

* Corresponding author, Tel: +98 21 66165522; Fax: +98 21 66000021
E-mail address: Saman@sharif.edu

of steady and incompressible flow, constant fluid properties and negligible energy dissipation and streamwise conduction effects is known as the Graetz problem, the one who originally solved this problem for a circular tube [8]. Since its original solution, the Graetz problem has served as an archetypal convective heat transfer problem both from a process modeling and an educational point of view. The Graetz problem for a microchannel has gained interest because of its fundamental importance in microfluidic problems such as the analysis and design of micro heat exchangers. Barron et al. [9] and Ameel et al. [10] have extended the Graetz problem to slip flow through a microtube with uniform temperature and uniform heat flux boundary conditions, respectively. Thermally developing laminar slip flow forced convection in rectangular microchannels has been studied by Yu and Ameel [11] by applying a modified generalized integral transform technique to solve the energy equation, assuming hydrodynamically fully developed flow.

Viscous dissipation effects are typically only significant for high viscous flows or in presence of high gradients in velocity distribution. In macroscale, such high gradients occur in high velocity flows. However, in microscale devices such as microchannels, because of small dimensions, such high gradients may occur even for low velocity flows. So, for microchannels the viscous dissipation should be taken into consideration. Viscous dissipation causes the variation in the temperature distributions by behaving like an energy source due to a considerable power generation induced by the shear stress, which, consequently, affects heat transfer rates. The effects of viscous dissipation on the temperature field and ultimately on the friction factor have been investigated by Koo and Kleinstreuer [12,13], using dimensional analysis and experimentally validated computer simulations. It was found that ignoring viscous dissipation could affect accurate flow simulations and measurements in microconduits. Aydin and Avci [4,5] have considered the effects of viscous heating in their studies. They also analytically studied slip flow heat transfer in a microannulus for the special case of one wall being adiabatic and the other having constant heat flux, considering viscous heating effects [14]. Viscous dissipation effect on fully developed slip flow forced convection in rectangular microchannels with constant wall heat flux has been studied by Aynor et al. [15]. Extended Graetz problem including viscous dissipation for a microtube was studied by Tunc and Bayazitoglu [16] using integral transform method. The two boundary conditions of constant wall temperature and constant wall heat flux were considered in the study. Similar study but for a slit microchannel with constant wall temperature was undertaken by Chen [17]. Aydin and Avci [18] numerically investigated thermally developing rarefied gas flow in a microchannel between two parallel plates by taking into account the influences of viscous heating for two different boundary conditions of constant wall temperature and constant wall heat flux.

Besides the analysis based on the basic conservation laws, the second law analysis is crucial in understanding the entropy generation attributed to the thermodynamic irreversibility, which is useful for studying the optimum operating conditions in designing a system with less entropy and destruction of available work (exergy), in accordance to the Gouy-Stodola theorem [19] stating that the lost available work is directly proportional to the entropy generation. Bejan [19,20] referred this method of engineering research as Entropy Generation Minimization (EGM) and discussed its derivations and applications in a vast coverage of applied thermal engineering. Nowadays, second law analysis of thermofluid systems has become a prominent topic in thermal engineering.

Despite the fact that there are numerous works related to second law analysis of macroscale devices, unfortunately the open literature shows very small number of papers that deal with entropy generation in microdevices. To the authors' best knowledge, the first thermodynamics analysis work considering rarefaction effects in microchannels has been performed by Haddad et al. [21]. They numerically investigated the entropy generation due to developing laminar forced convection through parallel plate microchannels with the boundary condition of constant wall temperature. Avci and Aydin [22] applied the second law analysis considering constant wall heat flux for two different microgeometries, namely, microtube and microducts, between two parallel plates. Hydrodynamically and thermally fully developed slip flow with constant properties was examined, using the previously obtained velocity and temperature profiles. Hooman [23] presented closed form solutions for fully developed temperature distribution and entropy generation due to forced convection in two above mentioned cross sections for two different thermal boundary conditions, being isothermal and isoflux walls. In a recent study, Sadeghi et al. [24] performed the second law of thermodynamics analysis for steady state hydrodynamically and thermally fully developed laminar gas flow in annulus microchannels with constant wall heat fluxes.

In the present study, the objective is to analytically investigate the entropy generation in thermally developing hydrodynamically fully developed laminar forced convection through a slit microchannel with constant wall heat fluxes. The rarefaction effects are taken into consideration using first order slip boundary conditions. Viscous heating is also included for either the wall cooling or the wall heating case. Using fully developed velocity profile, the energy equation is solved by means of integral transform. The interactive influences of rarefaction, viscous dissipation and the group parameter on entropy generation rates are shown in graphical form and also discussed in detail.

NOMENCLATURE

Be	Bejan number $[= N_{HT}/N_S]$
Br	Brinkman number $[= \mu U^2/qH]$
c_p	specific heat at constant pressure $[\mathrm{kJkg^{-1}K^{-1}}]$
D_h	hydraulic diameter of channel $[= 4H]$

F_m momentum accommodation coefficient
F_t thermal accommodation coefficient
h heat transfer coefficient [$\mathrm{Wm^{-2}K^{-1}}$]
H half of channel height [m]
k thermal conductivity [$\mathrm{Wm^{-1}K^{-1}}$]
Kn Knudsen number [$= \lambda/D_h$]
N normalization integral [Eq. (17)]
N_{FF} entropy generation number related to fluid friction
N_{HT} entropy generation number related to heat transfer
N_S entropy generation number, total [$= S_G/S_{G,C}$]
$N_{S,av}$ average entropy generation number
Nu Nusselt number [$= hD_h/k$]
p pressure [Pa]
Pr Prandtl number [$= \nu/\alpha$]
q wall heat flux [$\mathrm{Wm^{-2}}$]
Re Reynolds number [$= UD_h/\nu$]
S_G entropy generation rate [$\mathrm{Wm^{-3}K^{-1}}$]
$S_{G,C}$ characteristic entropy generation rate [$\mathrm{Wm^{-3}K^{-1}}$]
T temperature [K]
u axial velocity [$\mathrm{ms^{-1}}$]
U mean velocity [$\mathrm{ms^{-1}}$]
x axial coordinate [m]
y transverse coordinate [m]

Greek symbols

α thermal diffusivity [$\mathrm{m^2s^{-1}}$]
β eigenvalue
γ heat capacity ratio
η normal direction exiting the wall [m]
θ dimensionless temperature [Eq. (6)]
λ gas mean free path [m]
μ dynamic viscosity [$\mathrm{kgm^{-1}s^{-1}}$]
ν kinematic viscosity [$\mathrm{m^2s^{-1}}$]
φ auxiliary variable [Eq. (10)]
Φ transformed form of φ [Eq. (18)]
ψ eigenfunction
Ω dimensionless temperature difference [$= qH/kT_R$]

Subscripts

b bulk
R reference
s fluid property at solid surface
w wall
x local
0 inlet
∞ fully developed flow property

Superscript

$*$ dimensionless variable

2 SLIP VELOCITY AND TEMPERATURE JUMP

Due to velocity and temperature discontinuities on boundary, the fluid particles adjacent to the solid surface no longer attain the velocity and temperature of the solid surface. Therefore, the fluid particles have a tangential velocity, which is the slip velocity and a finite temperature difference, which is the temperature jump, at the solid surface. Using first order slip boundary conditions, the slip velocity and temperature jump are respectively expressed as [25]

$$u_s = \frac{2-F_m}{F_m} KnD_h \left(\frac{\partial u}{\partial \eta}\right)_w \tag{1}$$

$$T_s - T_w = \frac{2-F_t}{F_t}\frac{2\gamma}{1+\gamma}\frac{KnD_h}{Pr}\left(\frac{\partial T}{\partial \eta}\right)_w \tag{2}$$

where u_s and T_s are the velocity and temperature of the gas at the wall, respectively, T_w is the wall temperature, η is the normal direction exiting the wall, F_m is the tangential momentum accommodation coefficient and F_t is the thermal accommodation coefficient. The accommodation coefficients depend on various parameters that affect surface interaction, such as the magnitude and the direction of the velocity. It is shown that these coefficients are reasonably constant for a given gas and surface combination [26]. For light gases the accommodation coefficients may differ significantly from unity, while for heavy gases they are close to unity. If one deals with a sufficiently heavy gas and with an ordinarily contaminated surface, one may assume the values of accommodation coefficients to be unity [27]. According to Hadjiconstantinou [28], for most engineering applications the values of accommodation coefficients are close to unity.

3 MATHEMATICAL FORMULATION

The laminar hydrodynamically fully developed forced convection in a slit microchannel is considered. Geometry of the physical problem with the coordinate system is shown in Fig. 1. Because of symmetry, the analysis is restricted to the upper half domain of the channel. The fully developed velocity profile in dimensionless form can be determined from the momentum equation by employing the velocity slip condition, which modifies the Hagen-Poiseuille velocity profile, and the resulting profile becomes

$$u^*(y^*) = \frac{3}{2}\left(\frac{1+8\frac{2-F_m}{F_m}Kn - y^{*2}}{1+12\frac{2-F_m}{F_m}Kn}\right) \tag{3}$$

in which $y^* = y/H$, $u^* = u/U$ and U is the mean velocity.

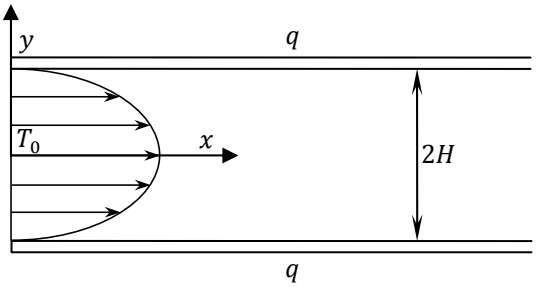

Fig. 1 Schematic of the slit microchannel and coordinate system.

3.1 First Law Analysis

It is assumed that temperature of the fluid entering the channel is uniform at $T = T_0$. Neglecting the axial conduction, the energy equation may be written as

$$u\frac{\partial T}{\partial x} = \alpha\frac{\partial^2 T}{\partial y^2} + \frac{\nu}{c_p}\left(\frac{\mathrm{d}u}{\mathrm{d}y}\right)^2 \tag{4}$$

and relevant boundary conditions are

$$\left(\frac{\partial T}{\partial y}\right)_{(x,0)} = 0 \tag{5a}$$

$$k\left(\frac{\partial T}{\partial y}\right)_{(x,H)} = q \tag{5b}$$

$$T_{(0,y)} = T_0 \tag{5c}$$

In order to generalize the solution, the energy equation and relevant boundary conditions are made dimensionless, using the following dimensionless parameters, besides those introduced previously

$$\theta = \frac{T - T_0}{\frac{qH}{k}} \quad , \quad x^* = \frac{x}{RePrD_h} \tag{6}$$

The energy equation then is modified into the following dimensionless form

$$\frac{3\left(1 + 8\frac{2-F_m}{F_m}Kn - y^{*2}\right)}{32\left(1 + 12\frac{2-F_m}{F_m}Kn\right)}\frac{\partial\theta}{\partial x^*} = \frac{\partial^2\theta}{\partial y^{*2}} + \frac{9Br}{\left(1 + 12\frac{2-F_m}{F_m}Kn\right)^2}y^{*2} \tag{7}$$

where the Brinkman number is defined as

$$Br = \frac{\mu U^2}{qH} \tag{8}$$

The Brinkman number is the criterion which shows the importance of viscous dissipation relative to the other terms of the energy equation. The thermal boundary conditions in the dimensionless form are written as

$$\left(\frac{\partial\theta}{\partial y^*}\right)_{(x^*,0)} = 0 \tag{9a}$$

$$\left(\frac{\partial\theta}{\partial y^*}\right)_{(x^*,1)} = 1 \tag{9b}$$

$$\theta_{(0,y^*)} = 0 \tag{9c}$$

Since the boundary conditions are non homogenous, therefore, a new variable φ is introduced, such that

$$\varphi(x^*, y^*) = \theta(x^*, y^*) - \theta_\infty(x^*, y^*) \tag{10}$$

where the fully developed temperature profile is simply derived as

$$\theta_\infty(x^*, y^*) = \frac{c_1}{2}\left(y^{*2} - 1\right) - \frac{c_2}{12}\left(y^{*4} - 1\right) + c_3\left(\frac{c_1}{3} - \frac{c_2}{15}\right) - c_4\left(\frac{c_1}{15} - \frac{c_2}{63}\right) + 16\left[1 + \frac{3Br}{\left(1 + 12\frac{2-F_m}{F_m}Kn\right)^2}\right]x^* \tag{11}$$

with

$$\left(\frac{\partial\theta_\infty}{\partial y^*}\right)_{(x^*,0)} = 0 \tag{12a}$$

$$\left(\frac{\partial\theta_\infty}{\partial y^*}\right)_{(x^*,1)} = 1 \tag{12b}$$

where

$$c_1 = \frac{1 + 8\frac{2-F_m}{F_m}Kn}{1 + 12\frac{2-F_m}{F_m}Kn}\left[\frac{3}{2} + \frac{9Br}{2\left(1 + 12\frac{2-F_m}{F_m}Kn\right)^2}\right]$$

$$c_2 = \frac{3}{2\left(1 + 12\frac{2-F_m}{F_m}Kn\right)} + \frac{9Br}{\left(1 + 12\frac{2-F_m}{F_m}Kn\right)^2} + \frac{9Br}{2\left(1 + 12\frac{2-F_m}{F_m}Kn\right)^3}$$

$$c_3 = \frac{3\left(1 + 8\frac{2 - F_m}{F_m}Kn\right)}{2\left(1 + 12\frac{2 - F_m}{F_m}Kn\right)} \quad , \quad c_4 = \frac{3}{2\left(1 + 12\frac{2 - F_m}{F_m}Kn\right)} \tag{13}$$

The following equation system, which is obtained after the substitution of $\theta = \varphi + \theta_\infty$ into the energy equation, is satisfied by φ

$$\frac{3\left(1 + 8\frac{2 - F_m}{F_m}Kn - y^{*2}\right)}{32\left(1 + 12\frac{2 - F_m}{F_m}Kn\right)}\frac{\partial\varphi}{\partial x^*} = \frac{\partial^2\varphi}{\partial y^{*2}} \tag{14a}$$

$$\left(\frac{\partial\varphi}{\partial y^*}\right)_{(x^*,0)} = 0 \tag{14b}$$

$$\left(\frac{\partial\varphi}{\partial y^*}\right)_{(x^*,1)} = 0 \tag{14c}$$

$$\varphi_{(0,y^*)} = -\theta_{\infty(0,y^*)} \tag{14d}$$

The finite integral transform method [29], a straightforward and very general technique for the solution of Graetz type channel flow problems, is applied to solve the present heat transfer problem. To begin with, an integral transform pair is developed by considering an eigenvalue problem appropriate for the present problem. Next, by transformation, the partial derivative with respect to y^* is removed from Eq. (14a), reducing it to an ordinary differential equation. Then the resulting ODE is solved subject to the transformed initial condition. Finally, φ is immediately obtainable from the inversion formula. Based on the method of separation of variables, an appropriate eigenvalue problem is given by

$$\frac{\mathrm{d}^2\psi}{\mathrm{d}y^{*2}} + \beta_m^2\left(1 + 8\frac{2 - F_m}{F_m}Kn - y^{*2}\right)\psi = 0 \tag{15a}$$

$$\left(\frac{\mathrm{d}\psi}{\mathrm{d}y^*}\right)_{(0)} = 0 \tag{15b}$$

$$\left(\frac{\mathrm{d}\psi}{\mathrm{d}y^*}\right)_{(1)} = 0 \tag{15c}$$

where $\psi(\beta_m, y^*)$'s and β_m's are the eigenfunctions and eigenvalues, respectively. Since the above eigenvalue problem constitutes a Sturm-Liouville problem, the eigenfunctions satisfy the following orthogonality condition

$$\int_0^1 \left(1 + 8\frac{2 - F_m}{F_m}Kn - y^{*2}\right)\psi(\beta_m, y^*)\psi(\beta_n, y^*)\mathrm{d}y^* = \begin{cases} 0 & \text{for } m \neq n \\ N(\beta_m) & \text{for } m = n \end{cases} \tag{16}$$

where the normalization integral $N(\beta_m)$ is calculated from the following formula

$$N(\beta_m) = \int_0^1 \left(1 + 8\frac{2 - F_m}{F_m}Kn - y^{*2}\right)[\psi(\beta_m, y^*)]^2\mathrm{d}y^* \tag{17}$$

Consequently, the integral transform pair with respect to the y^* variable is defined as

Transform:

$$\Phi(\beta_m, x^*) = \int_0^1 \left(1 + 8\frac{2 - F_m}{F_m}Kn - y^{*2}\right)\psi(\beta_m, y^*)\varphi(x^*, y^*)\mathrm{d}y^* \tag{18}$$

Inversion:

$$\varphi(x^*, y^*) = \sum_{m=1}^{\infty}\frac{\psi(\beta_m, y^*)}{N(\beta_m)}\Phi(\beta_m, x^*) \tag{19}$$

The next step in the solution is solving the eigenvalue problem by the method of Frobenius. Assuming the function $\psi(\beta_m, y^*)$ to be a power series gives

$$\psi(\beta_m, y^*) = \sum_{j=0}^{\infty} a_j(\beta_m){y^*}^j \tag{20}$$

From the first boundary condition of eigenvalue problem (15), it is evident that $a_1 = 0$. After substituting the series (20) into Eq. (15a), we obtain

$$a_2 = -\frac{\beta_m^2\left(1 + 8\frac{2 - F_m}{F_m}Kn\right)}{2}a_0$$

$$a_j = \begin{cases} 0 & \text{odd } j \geq 3 \\ \frac{\beta_m^2}{j(j-1)}\left[a_{j-4} - a_{j-2}\left(1 + 8\frac{2 - F_m}{F_m}Kn\right)\right] & \text{even } j \geq 4 \end{cases} \tag{21}$$

a_0 will appear as an additive constant at all steps. Hence, without loss of generality, we can assume a_0 to be 1 as it will not affect the shape of the temperature profile and gradients at the wall. So, $\psi(\beta_m, y^*)$ and its derivative with respect to y^* can be written as

$$\psi(\beta_m, y^*) = 1 + a_2 y^{*2} + a_4 y^{*4} + \cdots \tag{22a}$$

$$\frac{\mathrm{d}\psi(\beta_m, y^*)}{\mathrm{d}y^*} = 2a_2 y^* + 4a_4 y^{*3} + \cdots \tag{22b}$$

The second boundary condition of eigenvalue problem, Eq. (15c), is used to obtain eigenvalues. By substituting Eq. (22b) into Eq. (15c), we come up with

$$\sum_{j=2,4,\cdots}^{\infty} j a_j = 0 \tag{23}$$

Equation (23) may be rewritten by combining the coefficients of the terms containing the same power of β_m as

$$\sum_{k=1}^{\infty} b_k \beta^{2k} = b_1\beta^2 + b_2\beta^4 + \cdots = 0 \tag{24}$$

By numerically solving Eq. (24), the eigenvalues, β_m's are obtained. After solving the eigenvalue problem, we now take the integral transform of Eq. (14a) by the application of the transform (18). The transformation process starts with the operation on both terms of Eq. (14a) by the operator $\int_0^1 \psi(\beta_m, y^*)\,\mathrm{d}y^*$ to obtain

$$\frac{3}{32\left(1 + 12\frac{2-F_m}{F_m}Kn\right)}\int_0^1 \left(1 + 8\frac{2-F_m}{F_m}Kn - y^{*2}\right)\psi(\beta_m, y^*)\frac{\partial \varphi}{\partial x^*}\mathrm{d}y^* = \int_0^1 \psi(\beta_m, y^*)\frac{\partial^2 \varphi}{\partial y^{*2}}\mathrm{d}y^* \tag{25}$$

The term in the RHS of Eq. (25) is evaluated by integrating it by parts twice and utilizing the eigenvalue problem and the dimensionless boundary conditions of Eq. (14). Next, using the transform formula, we can obtain the following ordinary differential equation

$$\frac{\mathrm{d}\Phi_m}{\mathrm{d}x^*} + \frac{32\left(1 + 12\frac{2-F_m}{F_m}Kn\right)}{3}\beta_m^2\Phi_m = 0 \tag{26}$$

The solution to Eq. (26) is given by

$$\Phi_m = A_m e^{-B_m x^*} \tag{27}$$

where

$$B_m = \frac{32\left(1 + 12\frac{2-F_m}{F_m}Kn\right)}{3}\beta_m^2 \tag{28}$$

and A_m which is the integral transformation of the initial condition has the following form

$$A_m = -\int_0^1 \left(1 + 8\frac{2-F_m}{F_m}Kn - y^{*2}\right)\left[\frac{c_1}{2}\left(y^{*2} - 1\right) - \frac{c_2}{12}\left(y^{*4} - 1\right) + c_3\left(\frac{c_1}{3} - \frac{c_2}{15}\right) - c_4\left(\frac{c_1}{15} - \frac{c_2}{63}\right)\right]\psi(\beta_m, y^*)\mathrm{d}y^* \tag{29}$$

Hence, the transformed φ can be written as

$$\Phi_m = -\left\{\int_0^1 \left(1 + 8\frac{2-F_m}{F_m}Kn - y^{*2}\right)\left[\frac{c_1}{2}\left(y^{*2} - 1\right) - \frac{c_2}{12}\left(y^{*4} - 1\right) + c_3\left(\frac{c_1}{3} - \frac{c_2}{15}\right) - c_4\left(\frac{c_1}{15} - \frac{c_2}{63}\right)\right]\psi(\beta_m, y^*)\mathrm{d}y^*\right\} e^{-\frac{32\left(1+12\frac{2-F_m}{F_m}Kn\right)}{3}\beta_m^2 x^*} \tag{30}$$

By introducing Eq. (30) into the inversion formula, $\varphi(x^*, y^*)$ becomes

$$\varphi(x^*, y^*) = -\sum_{m=1}^{\infty} \frac{\psi(\beta_m, y^*)}{\int_0^1 \left(1 + 8\frac{2-F_m}{F_m}Kn - y^{*2}\right)[\psi(\beta_m, y^*)]^2\mathrm{d}y^*}\left\{\int_0^1 \left(1 + 8\frac{2-F_m}{F_m}Kn - y^{*2}\right)\left[\frac{c_1}{2}\left(y^{*2} - 1\right) - \frac{c_2}{12}\left(y^{*4} - 1\right) + c_3\left(\frac{c_1}{3} - \frac{c_2}{15}\right) - c_4\left(\frac{c_1}{15} - \frac{c_2}{63}\right)\right]\psi(\beta_m, y^*)\mathrm{d}y^*\right\} e^{-\frac{32\left(1+12\frac{2-F_m}{F_m}Kn\right)}{3}\beta_m^2 x^*} \tag{31}$$

Finally, the temperature distribution is obtained by adding θ_∞ to φ. Once the temperature distribution is obtained, the quantities of physical interest, including the bulk temperature of the fluid and the heat transfer rate can be obtained. The dimensionless bulk temperature can be expressed as

$$\theta_b = \int_0^1 u^*(y^*)\theta(x^*, y^*)\mathrm{d}y^* \tag{32}$$

The heat transfer rate can be expressed in terms of the local Nusselt number as

$$Nu_x = \frac{h_x D_h}{k} = \frac{qD_h}{k(T_w - T_b)}$$

$$= \frac{4}{\theta_s - \theta_b + \frac{2-F_t}{F_t}\frac{8\gamma}{1+\gamma}\frac{Kn}{Pr}} \tag{33}$$

3.2 Second Law Analysis

Entropy is generated due to the presence of irreversibility, and entropy generation is adopted as a quantitative measure of the irreversibility associated with a process. Flow and heat transfer processes inside the microchannel are irreversible. The non-equilibrium conditions arise due to the exchange of energy and momentum within the fluid and at solid boundaries, thus resulting in entropy generation. A part of the entropy production is due to the heat transfer in the direction of finite temperature gradients and the other part of entropy production arises due to the fluid friction. According to Bejan [20], the volumetric rate of entropy generation can be derived as

$$S_G = \frac{k}{T_R^2}\left(\frac{\partial T}{\partial y}\right)^2 + \frac{\mu}{T_R}\left(\frac{\mathrm{d}u}{\mathrm{d}y}\right)^2 \tag{34}$$

where T_R is the absolute reference temperature. Equation (34) can be made dimensionless to get entropy generation number N_S:

$$N_S = \frac{S_G}{S_{G,C}} = \left(\frac{\partial \theta}{\partial y^*}\right)^2 + \frac{Br}{\Omega}\left(\frac{\mathrm{d}u^*}{\mathrm{d}y^*}\right)^2 = N_{HT} + N_{FF} \tag{35}$$

where the dimensionless temperature difference Ω and the characteristic entropy generation rate $S_{G,C}$ are as follows

$$\Omega = \frac{qH}{kT_R} \tag{36a}$$

$$S_{G,C} = \frac{q^2}{kT_R^2} \tag{36b}$$

The ratio of Brinkman number to dimensionless temperature difference Br/Ω is known as the group parameter. The group parameter is an important dimensionless number for irreversibility analysis. It determines the importance of viscous effects [20] and cannot be neglected in real flow situations. On the RHS of Eq. (35), N_{HT} represents entropy generation due to heat transfer and N_{FF} is the fluid friction contribution to entropy generation. Using dimensionless velocity and temperature distributions, entropy generation number becomes

$$N_S(x^*, y^*) = \left\{ -\sum_{m=1}^{\infty} \frac{\frac{\mathrm{d}\psi(\beta_m, y^*)}{\mathrm{d}y^*}}{\int_0^1 \left(1 + 8\frac{2-F_m}{F_m}Kn - y^{*2}\right)[\psi(\beta_m, y^*)]^2 \mathrm{d}y} \right.$$
$$+ 8\frac{2-F_m}{F_m}Kn - y^{*2}\Big)\Big[\frac{c_1}{2}\left(y^{*2}-1\right) - \frac{c_2}{12}\left(y^{*4}-1\right)$$
$$+ c_3\left(\frac{c_1}{3} - \frac{c_2}{15}\right)$$
$$- c_4\Big(\frac{c_1}{15}$$
$$\left. -\frac{c_2}{63}\Big)\Big]\psi(\beta_m, y^*)\mathrm{d}y^* \right\} e^{-\frac{32\left(1+12\frac{2-F_m}{F_m}Kn\right)}{3}\beta_m^2 x^*} + c_1 y^*$$
$$\left. -\frac{c_2}{3}y^{*3} \right\}^2 + \frac{9\frac{Br}{\Omega}}{\left(1 + 12\frac{2-F_m}{F_m}Kn\right)^2} y^{*2} \tag{37}$$

Note that $\partial\varphi/\partial y^*$ vanishes at $x^* \to \infty$, so, the entropy generation number of fully developed flow $N_{S,\infty}$ will be in the following form

$$N_{S,\infty}(y^*) = \left(c_1 y^* - \frac{c_2}{3}y^{*3}\right)^2 + \frac{9\frac{Br}{\Omega}}{\left(1 + 12\frac{2-F_m}{F_m}Kn\right)^2} y^{*2} \tag{38}$$

The average dimensionless entropy generation over the cross section of the microchannel can be computed by the following integration

$$N_{S,av} = \frac{\int_0^1 N_S(x^*, y^*)\mathrm{d}y^*}{\int_0^1 \mathrm{d}y^*} = \int_0^1 N_S(x^*, y^*)\mathrm{d}y^* \tag{39}$$

In many engineering designs and energy optimization problems, the contribution of heat transfer entropy N_{HT} to overall entropy generation rate N_S which is known as Bejan number Be is needed. The Bejan number is so defined mathematically as

$$Be = \frac{N_{HT}}{N_S} \tag{40}$$

Clearly, the Bejan number ranges from 0 to 1. $Be = 0$ is the limit where the irreversibility is dominated by fluid friction effects and $Be = 1$ corresponds to the limit where the irreversibility due to heat transfer by virtue of finite temperature differences dominates. The contributions of both heat transfer and fluid friction to entropy generation are equal when $Be = 1/2$. Similar to entropy generation number, the fully developed Bejan number Be_∞ may be written as

$$Be_\infty(y^*)$$

$$= \frac{\left(c_1 y^* - \frac{c_2}{3} y^{*3}\right)^2}{\left(c_1 y^* - \frac{c_2}{3} y^{*3}\right)^2 + \frac{9\frac{Br}{\Omega}}{\left(1 + 12\frac{2-F_m}{F_m} Kn\right)^2} y^{*2}} \quad (41)$$

4 RESULTS AND DISCUSSION

The Knudsen number, the Brinkman number and the group parameter are the main parameters governing thermal transport characteristics in laminar slip flow forced convection through slit microchannels. Here, their interactive effects on transverse distributions of velocity and temperature and finally on entropy generation are analyzed. Without loss of generality, unless otherwise stated, the results are obtained using $Pr = 0.7$ and $\gamma = 1.4$. Also through this section the values of accommodation coefficients are assumed to be unity [9].

Figure 2 depicts transverse distribution of dimensionless velocity at different values of Knudsen number. As a result of slip conditions, slip velocity occurs at the wall. An increase in Kn results in an increase in the slip velocity at the wall, while according to mass conservation, the maximum velocity decreases. Note that as Knudsen number increases the velocity gradient becomes smaller, especially at the wall at which the maximum decrease occurs. Figure 3 shows the comparison between local Nusselt numbers obtained in present study against those given by Aydin and Avci [18] for $Kn = 0.025$ and $Pr = 0.71$ at different values of Brinkman number. It should be pointed out here that the definitions of dimensionless axial parameter, Knudsen number and Brinkman number in their study are different from ours. As seen, the results show quite good agreement.

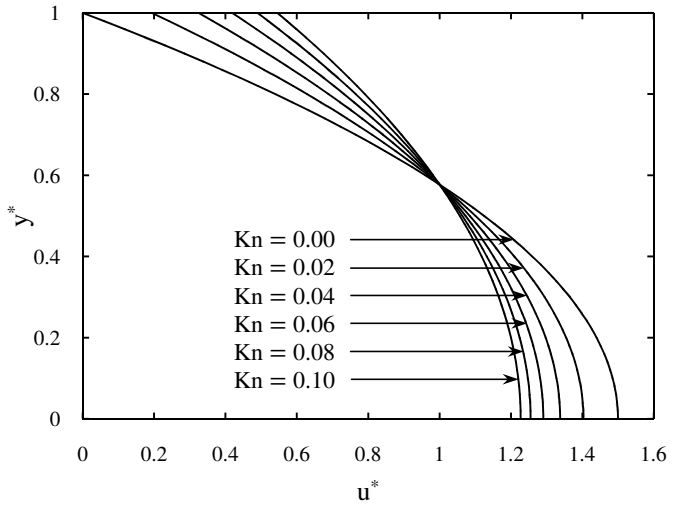

Fig. 2. Transverse distribution of dimensionless velocity at different values of Knudsen number.

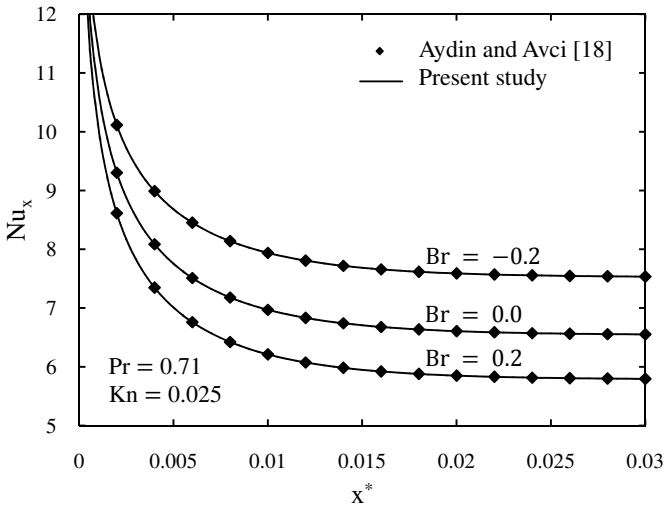

Fig. 3 Comparison between local Nusselt numbers obtained in present study against those given by Aydin and Avci [18].

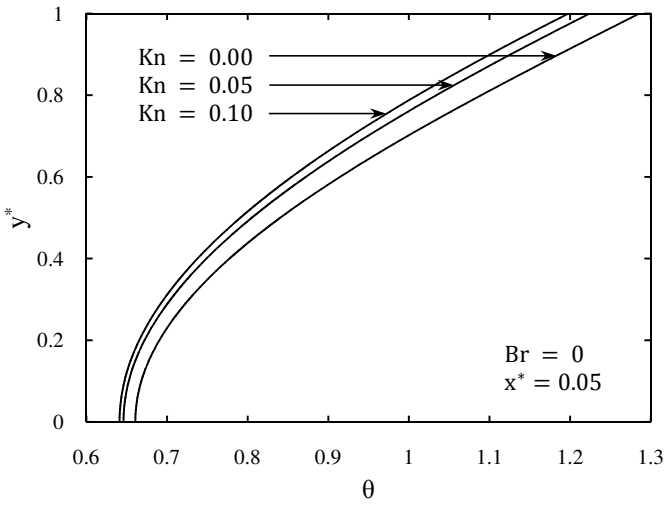

Fig. 4 Transverse distribution of dimensionless temperature in the absence of viscous heating.

Transverse distribution of dimensionless temperature of fully developed flow at different Knudsen numbers in the absence of viscous heating is illustrated in Fig. 4. As Knudsen number increases the dimensionless temperature decreases. The maximum and minimum decrements take place at the wall and centerline, respectively. Note that although the dimensionless temperature decreases, the dimensionless bulk temperature remains unchanged. This is because the viscous heating is absent and the total energy delivered to the flow by the wall is not dependent on Knudsen number. Transverse distribution of dimensionless temperature at different axial positions in the absence of viscous heating for no slip conditions is presented in Fig. 5. As x^* increases, the dimensionless temperature increases, which is an expected behavior. The existence of core flow which has not yet felt the presence of wall is seen for $x^* = 0.002$ and also at a smaller region for $x^* = 0.004$.

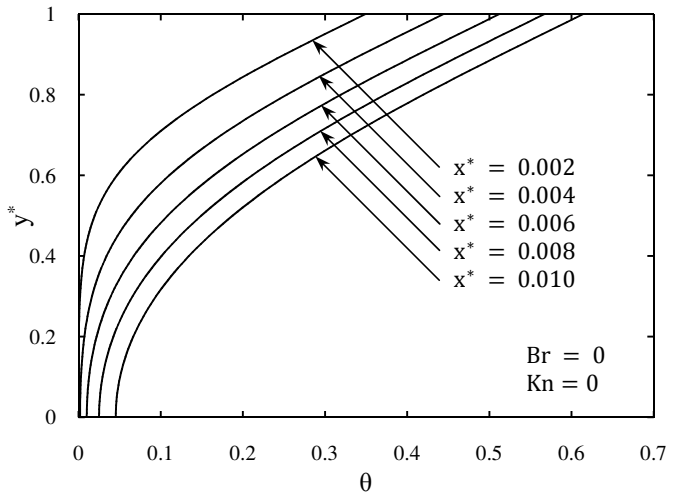

Fig. 5 Transverse distribution of dimensionless temperature at different axial positions in the absence of viscous heating.

In Fig. 6 transverse distribution of dimensionless temperature of fully developed flow at different values of Brinkman number is shown. Positive values of Brinkman number correspond to the wall cooling case where heat is transferred from the wall to the fluid, while the opposite is true for negative values of Brinkman. From the Figure, one can see that increasing values of Brinkman number lead to greater values of dimensionless temperature. This is due to the fact that as Brinkman number increases the energy generation due to viscous heating increases.

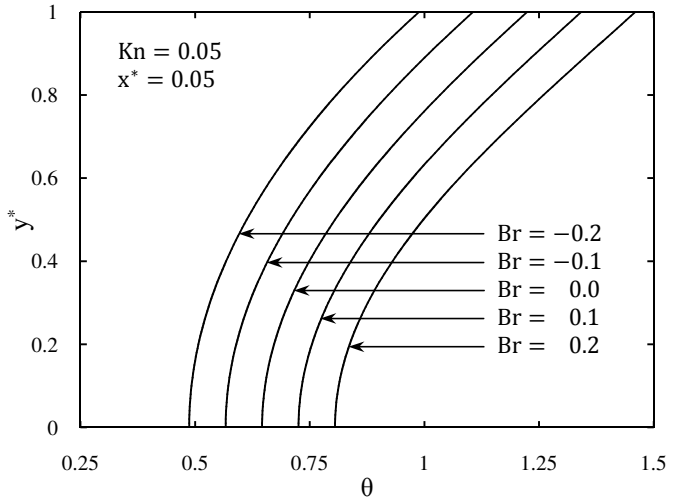

Fig. 6 Transverse distribution of dimensionless temperature at different values of Brinkman number.

Transverse distribution of N_S for $Br = 0.2$, $Kn = 0.05$ and $Br/\Omega = 0.25$ at different axial positions is depicted in Fig. 7. The distribution of N_S at $x^* \to \infty$ is obtained using Eq. (38). Entropy generation number attains its maximum value at the wall due to the presence of high velocity and temperature gradients. At centerline, at which velocity and temperature gradients are zero, the entropy generation number attains its minimum magnitude which is zero. As an expected behavior, the entropy generation number increases with increasing x^*. At the entrance the temperature distribution is uniform, except at the wall. So, the entropy generation is mainly due to fluid friction. As x^* is increased the extent of the core flow will shrink which this consequently leads to greater values of N_S. The corresponding Bejan number distribution for the above mentioned case is presented in Fig. 8. The Bejan number is greater for greater values of dimensionless axial coordinate. The Bejan number for $x^* = 0.002$ is zero in the vicinity of the centerline. This is the core flow which has not yet felt the presence of wall and the temperature is still uniform at T_0. For $x^* = 0.002$, the Bejan number attains its maximum value at the wall and reaches a local minimum at centerline. For greater values of x^* such as $x^* = 0.005$, the point of maximum Bejan number shifts a little to centerline, until it reaches centerline at fully developed conditions. Also the point of minimum Bejan number moves from centerline to the wall.

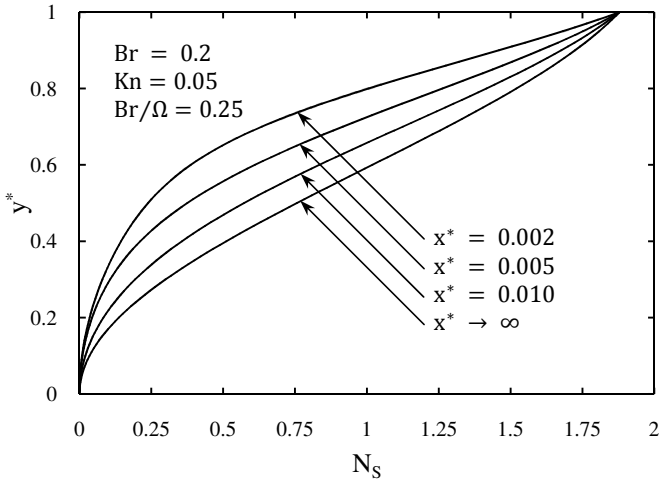

Fig. 7 Transverse distribution of N_S at different axial positions.

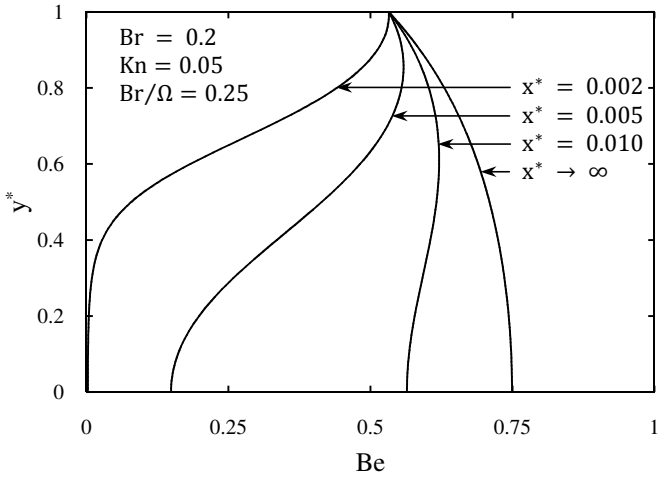

Fig. 8 Transverse distribution of Bejan number at different axial positions.

Figure 9 illustrates transverse distribution of $N_{S,\infty}$ for $Br = 0.2$ and $Br/\Omega = 0.25$ at different Knudsen numbers. As seen, to increase Knudsen number is to decrease entropy generation due to decreasing the velocity and temperature gradients. The maximum decrement takes place at the wall at which the maximum decrement of velocity slope occurs. The corresponding Bejan number distribution for the above mentioned case is illustrated in Fig. 10. Increasing Knudsen number leads to greater values of Bejan number which implies that the effect of Knudsen number on velocity distribution is greater than temperature distribution. The Bejan number distribution for high values of Knudsen number such as $Kn = 0.1$ is nearly uniform. This is due to the fact that slip conditions tend to unify the temperature and velocity profiles.

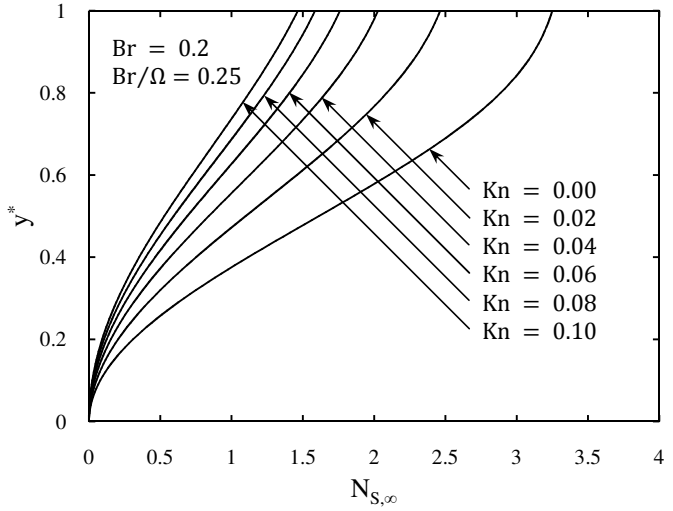

Fig. 9 Transverse distribution of $N_{S,\infty}$ at different Knudsen numbers.

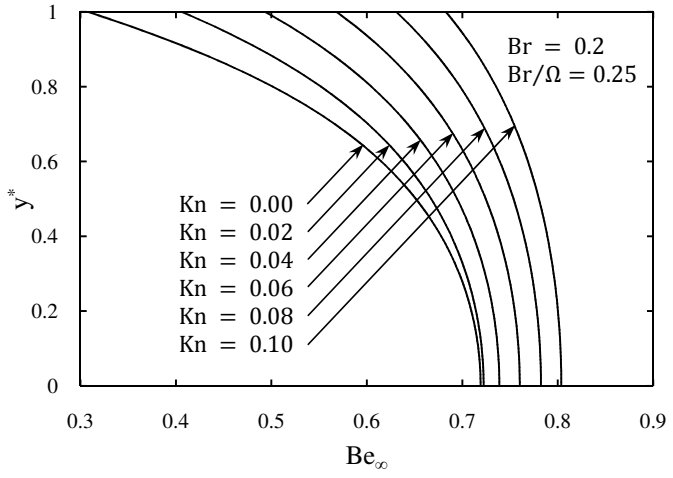

Fig. 10 Transverse distribution of fully developed Bejan number at different Knudsen numbers.

Figure 11 shows transverse distribution of $N_{S,\infty}$ for $Br = 0.2$ and $Kn = 0.05$ at different values of the group parameter. As expected, increasing values of the group parameter lead to greater values of $N_{S,\infty}$ due to increasing viscous effects. The maximum value of $N_{S,\infty}$ occurs at the wall, except for $Br/\Omega = 0$. In the absence of the fluid friction contribution to entropy generation, the point of maximum entropy generation number coincides with the point of maximum temperature gradient which for $Br = 0.2$ and $Kn = 0.05$ does not occurs at the wall. Transverse distribution of fully developed Bejan number at different values of the group parameter for $Br = 0.2$ and $Kn = 0.05$ is depicted in Fig. 12. For $Br/\Omega = 0$, the fluid friction contribution to entropy generation is zero. Bejan number is independent of transverse coordinate and equal to its maximum value which is unity. For other values of Br/Ω, the maximum and minimum values of Bejan number occur at centerline and the wall, respectively. A higher Br/Ω leads to a lower value of Bejan number due to increasing fluid friction effects.

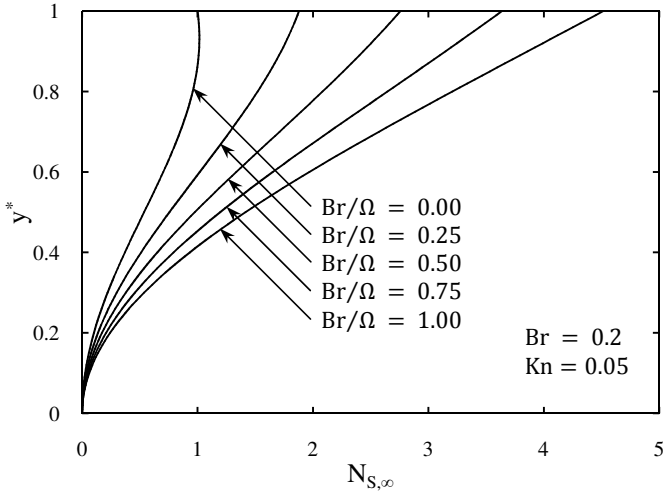

Fig. 11. Transverse distribution of $N_{S,\infty}$ at different group parameters.

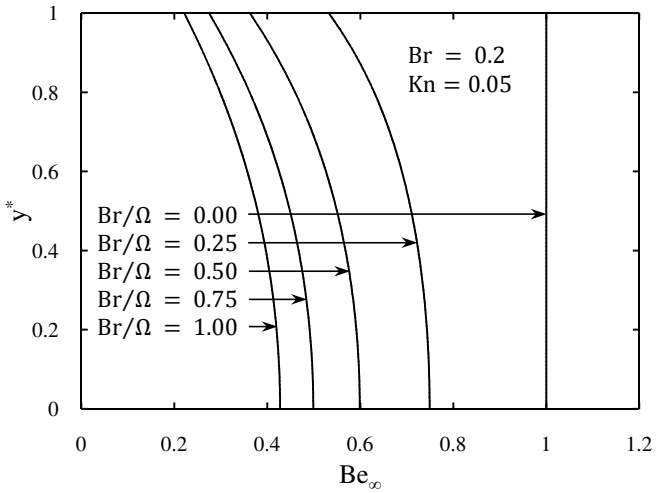

Fig. 12 Transverse distribution of fully developed Bejan number at different group parameters.

Downstream variation of average entropy generation number at different Knudsen numbers for $Br = 0.2$ and $Br/\Omega = 0.25$ is presented in Fig. 13. It can be seen that to increase Knudsen is to decrease average entropy generation number due to decreasing temperature and velocity slopes. The decrease of fully developed average entropy generation number for $Kn = 0.1$ with respect to no slip conditions is more than 60%. Moreover, $N_{S,av}$ increases with increasing values of x^*, until it reaches a constant value at fully developed conditions. The reason is that as flow is thermally being developed the region affected by the wall heat flux will grow and consequently attain greater temperature gradients. Figure 14 shows variation of average entropy generation number in the entrance region at different Brinkman numbers for for $Kn = 0.05$ and $Br/\Omega = 0.25$. A greater Brinkman number is accompanied by greater magnitudes of average entropy generation number, except at the entrance. At the entrance, entropy generation is mainly due to fluid friction effects and since viscous heating only affects temperature distribution, its effect on entropy generation is negligible. Effects of Br/Ω on average entropy generation number in the entrance region is illustrated in Fig. 15. Increasing Br/Ω results in higher magnitudes of $N_{S,av}$. The increment of average entropy generation number due to increasing values of the group parameter is constant for each axial position. This is because of linear dependency of entropy generation to Br/Ω.

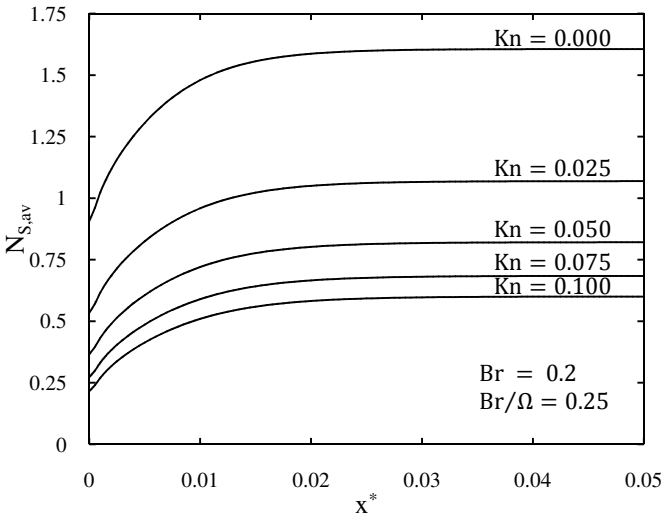

Fig. 13 Downstream variation of average entropy generation number at different Knudsen numbers.

5 CONCLUSIONS

We have analytically studied entropy generation in thermally developing forced convection through a slit microchannel. The analysis included the influence of the viscous dissipation in addition to the slip velocity and temperature jump prescriptions at the wall. Using fully developed velocity profile, the energy equation was solved by means of integral transform. An expression for entropy generation number in the form of an infinite series was obtained. For fully developed conditions, closed form solutions were presented for entropy generation number and Bejan number. From the results it is disclosed that the entropy generation decreases as Knudsen number increases. This is due to the fact that slip conditions tend to unify the velocity and temperature profiles. Depending of the value of flow parameters, the decrease of average entropy generation number for $Kn = 0.1$ with respect to no slip conditions may be even more than 60%. The effect of increasing values of Brinkman number and the group parameter is to increase entropy generation. Also it is found that the average entropy generation number over the cross section of channel increases with increasing values of axial coordinate, until it reaches a constant value at fully developed conditions.

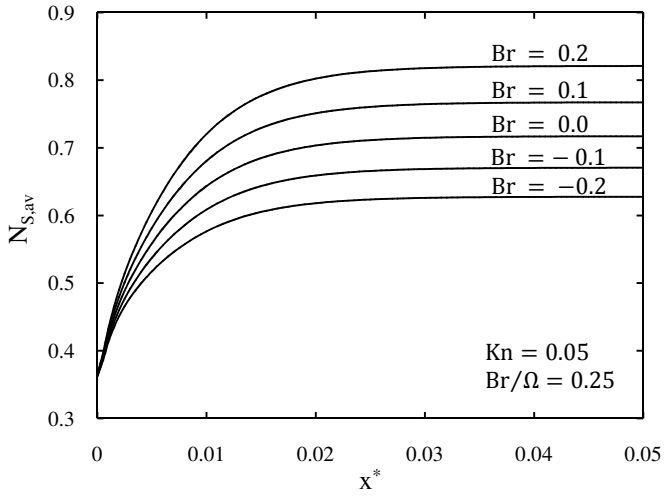

Fig. 14 Variation of average entropy generation number in the entrance region at different Brinkman numbers.

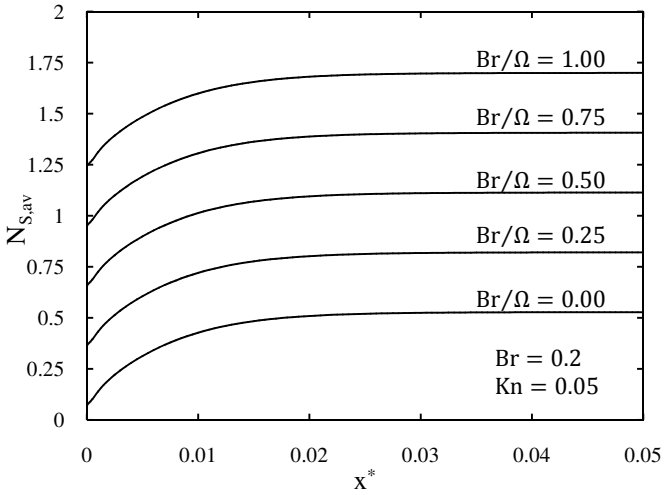

Fig. 15 Effects of Br/Ω on average entropy generation number in the entrance region.

6 REFERENCES

[1] Beskok, A., and Karniadakis, G.E., 1994, "Simulation of Heat and Momentum Transfer in Complex Micro-Geometries," *J. Thermophysics Heat Transfer*, 8, pp. 647–655.

[2] Liu, J., Tai, Y.C., and Ho, C.M., 1995, ''MEMS for Pressure Distribution Studies of Gaseous Flows in Microchannels,'' *Proceedings of IEEE, International Conference on Micro Electro Mechanical Systems*, Amsterdam, Netherlands, pp. 209–215.

[3] Hsieh ,S.S., Tsai, H.H., Lin, C.Y., Huang, C.F., and Chien, C.M., 2004, "Gas Flow in a Long Microchannel," *Int. J. Heat Mass Transfer*, 47, pp. 3877–3887.

[4] Aydin, O., and Avci, M., 2006, "Heat and Flow Characteristics of Gases in Micropipes," *Int. J. Heat Mass Transfer*, 49, pp. 1723–1730.

[5] Aydin O., and Avci M., 2007, "Analysis of Laminar Heat Transfer in Micro-Poiseuille Flow, *Int. J. Therm. Sci.*, 46, pp. 30–37.

[6] Duan, Z., and Muzychka, Y.S., 2008, "Slip Flow Heat Transfer in Annular Microchannels With Constant Heat Flux," *J. Heat Transfer*, 130(9), 092401.

[7] Tunc, G., and Bayazitoglu, Y., 2002, "Heat Transfer in Rectangular Microchannels," Int. J. Heat Mass Transfer, 45, pp. 765–773.

[8] Graetz, L., part 1, 1883, part 2, 1885, "Uber die Warmeleitungsfahigheit von Flussingkeiten," *Annalen der Physik und Chemie*, part 1, 18, pp. 79–94, part 2, 25, pp. 337–357.

[9] Barron, R.F., Wang, X., Ameel, T.A., and Warrington, R.O., 1997, ''The Graetz Problem Extended to Slip Flow,'' *Int. J. Heat Mass Transfer*, 40, 8, pp. 1817-1823.

[10] Ameel, T.A., Wang, X.M., Baron, R.F., and Warrington, R.O., 1997, "Laminar Forced Convection in a Circular Tube With Constant Heat Flux and Slip Flow," *Microscale Thermophys. Eng.*, 1(4), pp. 303–320.

[11] Yu, S., Ameel, T.A., 2001, "Slip Flow Heat Transfer in Rectangular Microchannels," *Int. J. Heat Mass Transfer*, 44, pp. 4225–4234.

[12] Koo, J., and Kleinstreuer, C., 2003, "Liquid Flow in Microchannels: Experimental Observations and Computational Analyses of Microfluidics Effects," *J. Micromechanics and Microengineering*, 13, pp. 568–579.

[13] Koo, J., and Kleinstreuer, C., 2004, "Viscous Dissipation Effects in Microtubes and Microchannels," *Int. J. Heat Mass Transfer*, 47, pp. 3159–3169.

[14] Avci, M., and Aydin, O., 2008, "Laminar Forced Convection Slip-Flow in a Micro-Annulus Between Two Concentric Cylinders," *Int. J. Heat Mass Transfer*, 51, pp. 3460–3467.

[15] Aynur, T.N., Kuddusi, L., and Egrican, N., 2006, "Viscous Dissipation Effect on Heat Transfer Characteristics of Rectangular Microchannels Under Slip Flow Regime and H1 Boundary Conditions," *Heat Mass Transfer*, 42, pp. 1093–1101.

[16] Tunc, G., and Bayazitoglu, Y., 2001, "Heat Transfer in Microtubes With Viscous Dissipation," *Int. J. Heat Mass Transfer*, 44, pp. 2395–2403.

[17] Chen, C.H., 2006, "Slip Flow Heat Transfer in a Microchannel With Viscous Dissipation," *Heat Mass Transfer*, 42, pp. 853–860.

[18] Aydin, O., and Avci, M., 2006, "Thermally Developing Flow in Microchannels," *J. Thermophysics Heat Transfer*, 20(3), pp. 628–632.

[19] Bejan, A., 1982, "Second-Law Analysis in Heat Transfer and Thermal Design," *Advances in Heat Transfer*, 15, pp. 1–58.

[20] Bejan, A., 1996, *Entropy Generation Minimization*, CRC Press, New York.

[21] Haddad, O., Abuzaid, M., and Al-Nimr, M., 2004, "Entropy Generation due to Laminar Incompressible Forced Convection Flow Through Parallel Plates Microchannel," *Entropy*, 6, 5, pp. 413–426.

[22] Avci, M. and Aydin, O., 2007, "Second Law Analysis of Heat and Fluid Flow in Microscale Geometries," *Int. J. Exergy*, 4, 3, pp. 286–301.

[23] Hooman, K., 2007, "Entropy Generation for Microscale Forced Convection: Effects of Different Thermal Boundary Conditions, Velocity Slip, Temperature Jump, Viscous Dissipation, and Duct Geometry," *Int. Comm. Heat Mass Transfer*, 34, pp. 945–957.

[24] Sadeghi, A., Asgarshamsi, A., and Saidi, M.H., 2009, "Second Law Analysis of Slip Flow Heat Transfer in Annulus Microchannel," *Proceedings of ASME Summer Heat Transfer Conference*, San Francisco, California.

[25] Beskok, A., Karniadakis, G.E., and Trimmer, W., 1996, "Rarefaction and Compressibility Effects in Gas Microflows," *J. Fluids Engrg.*, 118, pp. 448–456.

[26] Schaaf, S.A., 1963, "Mechanics of Rarefied Gases," Encyclopedia of Physics, Vol. Fluid Dynamics II, VII/2, Berlin, pp. 591–624.

[27] Sharipov, F., and Seleznev, V., 1998, "Data on Internal Rarefied Gas Flows," *J. Phys. Chem. Ref. Data*, 27(3), pp. 657–706.

[28] Hadjiconstantinou, N.G., 2006, "The Limits of Navier Stokes Theory and Kinetic Extensions for Describing Small Scale Gaseous Hydrodynamics," *Phys. Fluids*, 18, 111301.

[29] Bayazitoglu, Y., and Ozisik, M.N., 1980, "On the Solution of Graetz Type Problems With Axial Condition," *Int. J. Heat Mass Transfer*, 23, pp. 1399–1402.